Upper bound for the *s-d* exchange integral in *n*-(Ga,Mn)N:Si from magnetotransport studies

R. Adhikari,[1] W. Stefanowicz,[2] B. Faina,[1] G. Capuzzo,[1] M. Sawicki,[2] T. Dietl,[2,3,4,*] and A. Bonanni[1,†]

[1]*Institut für Halbleiter-und-Festkörperphysik, Johannes Kepler University, Altenbergerstrasse 69, A-4040 Linz, Austria*

[2]*Institute of Physics, Polish Academy of Sciences, al. Lotników 32/46, PL-02-668 Warszawa, Poland*

[3]*Institute of Theoretical Physics, Faculty of Physics, University of Warsaw, ul. Pasteura 5, PL-02-093 Warszawa, Poland*

[4]*WPI-Advanced Institute for Materials Research (WPI-AIMR), Tohoku University, 2-1-1 Katahira, Aoba-ku, Sendai 980-8577, Japan*

(Received 12 December 2014; revised manuscript received 10 April 2015; published 12 May 2015)

A series of recent magneto-optical studies pointed to contradicting values of the *s-d* exchange energy $N_0\alpha$ in Mn-doped GaAs and GaN as well as in Fe-doped GaN. Here, a strong sensitivity of weak-localization phenomena to symmetry-breaking perturbations (such as spin-splitting and spin-disorder scattering) is exploited to evaluate the magnitude of $N_0\alpha$ for *n*-type wurtzite (Ga,Mn)N:Si films grown by metalorganic vapor phase epitaxy. Millikelvin magnetoresistance studies and their quantitative interpretation point to $N_0\alpha < 40$ meV, a value at least 5 times smaller than the one found with similar measurements on, e.g., *n*-(Zn,Mn)O. It is shown that this striking difference in the values of the *s-d* coupling between *n*-type III-V and II-VI dilute magnetic semiconductors can be explained by a theory that takes into account the acceptor character of Mn in III-V compounds.

DOI: 10.1103/PhysRevB.91.205204 PACS number(s): 75.50.Pp, 71.70.Ej, 72.15.Rn, 72.80.Ey

I. INTRODUCTION

The existence of a strong *sp-d* interaction $-J\vec{s}\cdot\vec{S}_i$ between effective mass carriers with a spin $\vec{s}$ and a subsystem of spins $\vec{S}_i$ localized on magnetic impurities is characteristic of dilute magnetic semiconductors (DMSs) [1–3]. This interaction accounts for the giant Zeeman splitting of bands, spin-disorder scattering, the formation of magnetic polarons, and the mediation by itinerant carriers of ferromagnetic coupling between magnetic ions [1–4]. A strong sensitivity of quantum-localization phenomena to symmetry-breaking perturbations (such as spin-splitting and spin-disorder scattering) results in striking magnetotransport phenomena in DMSs [5]. In this work we exploit this sensitivity and demonstrate that the *s-d* exchange integral is surprisingly small in $Ga_{1-x}Mn_xN$:Si with low Mn content x. We explain this result in terms of a previously developed theoretical model [6] that links the reduction in the apparent *s-d* interaction to the acceptor character of Mn in GaN.

In the case of tetrahedrally bound semiconductors, the *sp-d* interaction is characterized by the two exchange integrals, $\alpha = \langle S|J|S\rangle$ and $\beta = \langle X|J|X\rangle$, where S and X stand for the periodic parts of the Bloch wave function (Kohn-Luttinger amplitudes), which respectively transform as atomic s and p_x orbitals under symmetry operations of the crystallographic point group [2,7].

If the bottom of the conduction band is formed by states derived from cation and anion s orbitals, spin-dependent effects involving electrons originate from the intra-atomic potential *s-d* exchange interaction. Indeed, the corresponding *s-d* exchange energy is 390 meV in the case of free Mn^{1+} ions [8], whereas in DMSs this value is subjected to an up to twofold reduction by a covalent admixture of the anion *s*-type wave function to the Kohn-Luttinger amplitude at the conduction band edge. In accord with this insight, the values of $N_0\alpha$ (where N_0 is the cation concentration) as determined from magneto-optics experiments are in the range $190 \lesssim N_0\alpha \lesssim 320$ meV for a series of paramagnetic II-VI compounds doped with Mn as well as with Cr, Fe, and Co [7,9]. These findings are in good quantitative agreement with *ab initio* studies for (II,Mn)VI DMSs [10,11]. At the same time, by employing the magneto-optical values of $N_0\alpha$ it was possible to quantitatively interpret the positive magnetoresistance originating from the influence of giant spin-splitting of the conduction band upon disorder-modified electron-electron interactions in paramagnetic *n*-type (Cd,Mn)Se [12], (Cd,Mn)Te [13,14], (Cd,Zn,Mn)Se [15], (Zn,Mn)O [16], and (Zn,Co)O [17] near the metal-to-insulator transition.

In contrast to this clear-cut situation, the physics of exchange coupling between conduction band electrons and magnetic impurities in III-V DMSs appears more complex. Here, *ab initio* computations predicted that the magnitudes of $N_0\alpha$ in (Ga,Mn)As and (Ga,Mn)N should be similar to those in (II,Mn)VI DMSs [10,18]. However, rather different values are implied by magneto-optical studies on dilute paramagnetic $Ga_{1-x}Mn_xAs$ ($x \leqslant 0.13\%$) grown by molecular beam epitaxy at high temperatures, which point to an *antiferromagnetic* $N_0\alpha = (-23 \pm 8)$ meV for photoelectrons at the band edge [19–21]. These data challenge the time-honored notion that the spin-dependent coupling between electrons and Mn spins in a tetrahedrally coordinated DMS originates from the necessarily ferromagnetic intra-atomic potential *s-d* exchange. This riddle was solved [6] by noting that for the Mn concentrations and growth conditions in question, Mn ions are accompanied by bound holes. In such a case, in addition to the *s-d* interaction, *s-p* exchange between electrons and bound holes is present and overcompensates the *s-d* coupling. Good agreement between experimental and theoretical values of $N_0\alpha$ was found without adjustable parameters [6]. This model explained also (i) the two orders of magnitude *longer* spin relaxation time of electrons in GaAs:Mn compared to GaAs:Ge, where only *s-p* exchange operates [22]; (ii) the crossover to a positive value $xN_0\alpha = (+2.3 \times 10^{-2})$ meV in presumably more compensated $Ga_{1-x}Mn_xAs$ samples

*dietl@ifpan.edu.pl
†alberta.bonanni@jku.at

($x \simeq 0.1\%$), in which electron spin-flip Raman scattering was observed [23]; and (iii) a much reduced spin-splitting found for electrons injected into InAs quantum dots containing a neutral Mn acceptor [24].

In the case of magnetically doped wurtzite (wz) GaN, exciton magnetospectroscopy [25–27] and magnetic circular dichroism [28] were employed to evaluate the *sp-d* exchange energies in films deposited by metalorganic vapor phase epitaxy (MOVPE). These methods provide the magnitude of $N_0(\beta - \alpha)$ rather accurately. If, however, all three fundamental excitons A, B, and C are resolved, some information on $N_0\alpha$ can also be obtained. By applying a multiparameter fitting procedure to magnetoreflectivity spectra the values $N_0\alpha = (0 \pm 100)$ and $(+100 \pm 200)$ meV were determined for $Ga_{1-x}Fe_xN$ ($x \leqslant 0.21\%$) and $Ga_{1-x}Mn_xN$ ($x \leqslant 0.9\%$), respectively [26,27]. The former was reassessed by examining excitonic magnetic circular dichroism for $Ga_{1-x}Fe_xN$ with $x = 0.2\%$, which resulted in $N_0\alpha = (+50 \pm 100)$ meV [28]. In contrast, results of more recent time-resolved Kerr rotation measurements that probe directly photoelectrons, not excitons, point to a standard value $N_0\alpha = (+230 \pm 20)$ meV for a series of $Ga_{1-x}Mn_xN$ films obtained by MOVPE with x up to 0.27% [29]. On the other hand, a much lower value $N_0|\alpha| = (14 \pm 4)$ meV was found by analyzing the effect of the electrons on the Mn^{2+} longitudinal relaxation time T_1 in compensated bulk *n*-type $Ga_{1-x}Mn_xN$ samples with $x \leqslant 0.2\%$ [30]. However, the interpretation of electron paramagnetic resonance data was carried out [30] neglecting possible effects of the relaxation-time bottleneck [31] that in the case of similar Landé factors of carriers and localized spins can increase the apparent value of T_1, leading to an underestimation of the *s-d* coupling energy $N_0|\alpha|$.

The above discussion indicates that the issue of the *s-d* interaction in (Ga,Mn)N, and more generally in III-V DMSs, is by no means settled. Here we present results of millikelvin magnetoconductance (MC) measurements on a series of *n*-type wz-(Ga,Mn)N:Si films grown by MOVPE. The studied samples have all nominally the same concentration of Si donors, $N_D \approx 10^{19}$ cm^{-3}, but different content x of Mn acceptors, so that the electron concentration diminishes with x down to $n = 1.4 \times 10^{18}$ for $x = 0.06\%$. The MC data are described in terms of a model that takes quantum-localization corrections into account [32–35], and which previously described successfully MC experiments on *n*-type II-VI DMSs [12–17] as well as on their nonmagnetic counterparts, i.e., zinc-blende CdTe:In [36] and wurtzite CdSe:In [12], ZnO:Al [16], and GaN:Si, as we reported recently [37]. In particular, we take here into account the influence of spin-splitting of the conduction band upon disorder-induced one-electron [33,35] and many-body interference phenomena [32–34]. Our present results indicate that the MC of $Ga_{1-x}Mn_xN$:Si is not markedly affected by *s-d* coupling. Their quantitative interpretation points to $N_0|\alpha| < 40$ meV. Thus, our data provide a new support to the theory [6] that assigns a reduction in the apparent magnitude of $N_0\alpha$ to repulsion of electrons by negatively charged Mn acceptors in *n*-type III-V DMSs.

II. SAMPLES AND EXPERIMENTAL

The GaN layers co-doped with Si and Mn have been grown in an AIXTRON 200RF horizontal tube metalorganic vapor phase epitaxy (MOVPE) reactor and deposited on a *c*-plane sapphire substrate using TMGa, $MnCp_2$, NH_3, and SiH_4 as precursors for Ga, Mn, N, and Si, respectively, with H_2 as carrier gas. After nitridation of the sapphire substrate, a low temperature nucleation layer is deposited at 540 °C and then annealed at 1040 °C. An insulating 1-μm-thick GaN:Mn buffer layer is grown at 1040 °C, Mn being introduced in order to compensate residual donors accounting for the *n*-type character of conductivity in GaN fabricated by MOVPE. Finally, a (Ga,Mn)N:Si layer with a thickness $d = 150$ nm is grown at 1000 °C. The Mn content x ranges from about 0.01 to 0.06% over the samples series, as determined by secondary ions mass spectroscopy (SIMS).

The samples S0–S3 considered here and listed in Table I are systematically characterized by atomic force microscopy (AFM), high-resolution x-ray diffraction (HRXRD), and high-resolution transmission electron microscopy (HRTEM). Information on the morphology of the sample surface is obtained from tapping-mode AFM performed with a VEECO Dimension 3100 AFM system. The (10×10) μm^2 scans reported in Figs. 1(a)–1(d) give values of the root mean square roughness (R_{rms}) of ≈1 nm for all samples considered and evidence a step-flow growth mode. The (40×40) μm^2 scans shown in Figs. 1(e)–1(h) provide for the R_{rms} values ranging from ≈3 nm for sample S0 to ≈6 nm for sample S3 with no spiral hillocks detected.

X-ray rocking curves (XRC) and reciprocal space maps (RSM) are measured using a PANalytical X'Pert PRO Materials Research Diffractometer (MRD) equipped with a hybrid monochromator with a 1/4° divergence slit. The diffracted beam is collected by a solid-state PixCel detector with a 9.1 mm antiscatter slit. The rocking curves—(ω-2θ) scans in Figs. 2(a) and 2(b)—are measured on the symmetric (0002) and asymmetric ($10\bar{1}5$) Bragg reflections of the wz-GaN crystal system. The full width at half maxima (FWHM) of the (0002) and ($10\bar{1}5$) diffraction peaks are listed in Table I. The values for symmetric (0002) reflection of all

TABLE I. FWHM of the symmetric and asymmetric diffraction peak, electron concentration n, mobility μ, parameter $k_F\ell$, and Mn concentration x as obtained from SIMS and from Hall measurements for the reference sample S0 (Ref. [37]) and for samples S1–S3.

Sample	FWHM (0002) (arcsec)	FWHM ($10\bar{1}5$) (arcsec)	n (10^{18}/cm^3)	μ (cm^2/Vs)	$k_F\ell$	x (%) SIMS	x (%) Hall
S0	150	239	12	140	4.6	<0.01	refr.
S1	149	264	7.3	139	3.3	≲0.01	0.011
S2	153	282	4.7	103	1.8	0.02	0.017
S3	142	257	1.4	102	0.8	0.06	0.024

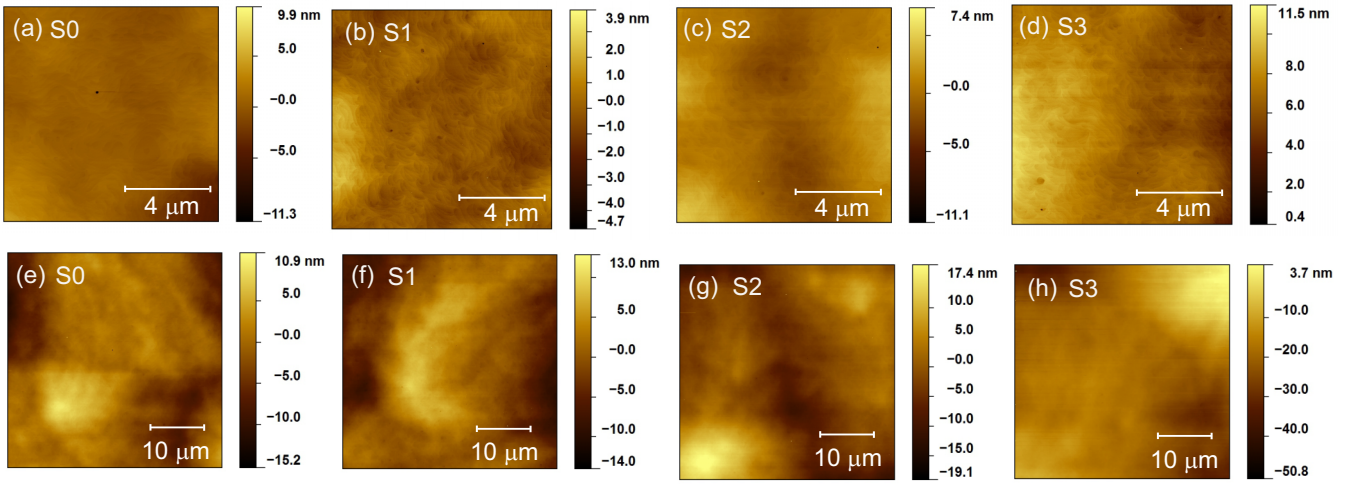

FIG. 1. (Color online) Upper panels: AFM images of (10×10) μm^2 scan areas for sample S0 (a), S1 (b), S2 (c), and S3 (d). Lower panels: AFM images of (40×40) μm^2 scan areas for sample S0 (e), S1 (f), S2 (g), and S3 (h).

the four samples is ≈150 arcsec while for the asymmetric $(10\bar{1}5)$ reflection vary between 239 arcsec and 282 arcsec, confirming the high crystallinity of the samples studied here [38]. In the RMSs represented in Figs. 2(c)–2(f) the slight horizontal broadening in the Q_x direction for the samples S1–S3 compared to S0 is to be assigned to sample tilt, finite lateral coherence length of mosaic blocks, and compositional fluctuations.

The HRTEM analysis does not reveal any secondary phases such as precipitates of Si_xN or Mn-rich compounds.

Hall bars with Ti/Au/Al/Ti/Au metallic contacts have been fabricated by conventional photolithography. Measurements of resistivity $\rho(T,B)$ as a function of temperature T and magnetic field B have been performed in a dedicated home-built helium cryostat and a dilution refrigerator down to 50 mK. To avoid the remanent magnetic field characteristic to superconducting magnets, weak-field measurements are carried out in a copper coil. The Hall coefficient $R_H = -\partial\rho_{xy}/\partial B$ at 50 K as a function of B up to 2 T is reported in Fig. 3 for the studied samples and there is no indication of nonlinear components.

The magnitudes of electron concentration n, mobility μ, product of Fermi wave vector and mean-free path, $k_F\ell$, obtained from Hall resistivity measurements at 5 K, and x as determined by SIMS are collected in Table I for the sample S0 discussed previously [37] and for the Mn-doped GaN:Si samples S1–S3 studied within the present work. For comparison, x values estimated from the Hall data according to $x(\text{Hall}) = [n(\text{S0}) - n]/N_0$ are also shown in Table I. It is assumed in this evaluation that the incorporation of Si donors is independent of the Mn acceptor density.

As seen, by co-doping with Mn acceptors we drive GaN:Si towards the metal-to-insulator transition occurring at $n \simeq 1\times10^{18}$ cm^{-3} in n-GaN [39]. In this range, the magnitude of the conductance is strongly affected by quantum-localization corrections that depend sensitively, according to theoretical expectations [32,34,35,40] and experimental studies [12–17], on the giant spin-splitting of the conduction band in DMSs.

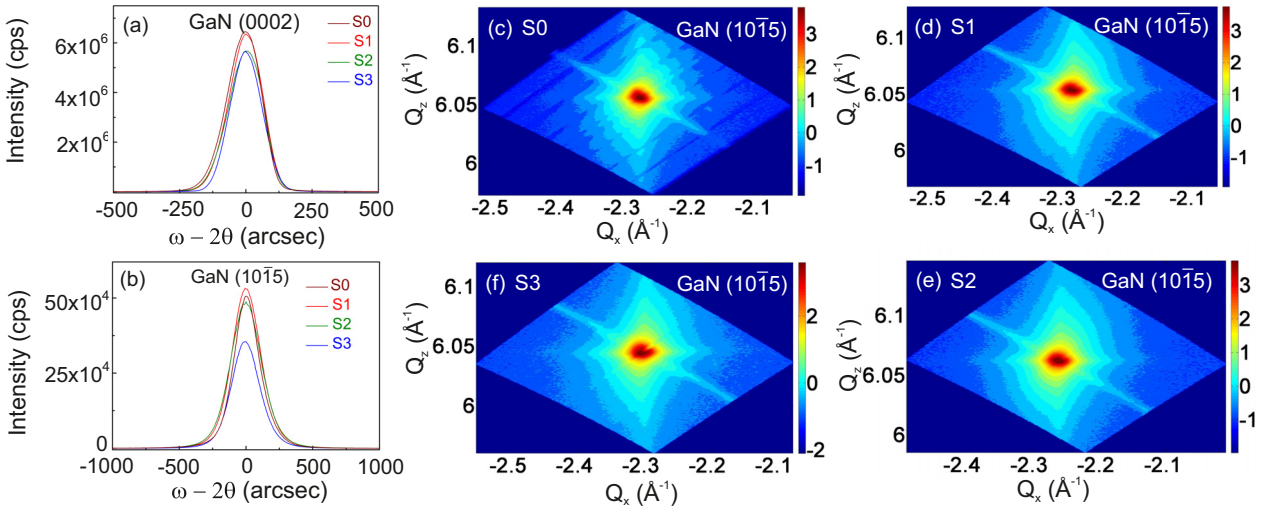

FIG. 2. (Color online) (a), (b) X-ray rocking curves for the symmetric (0002) and for the asymmetric $(10\bar{1}5)$ reflection, respectively. (c)–(f) Reciprocal space maps for the asymmetric $(10\bar{1}5)$ reflection of sample S0 (c), S1 (d), S2 (e), and S3 (f).

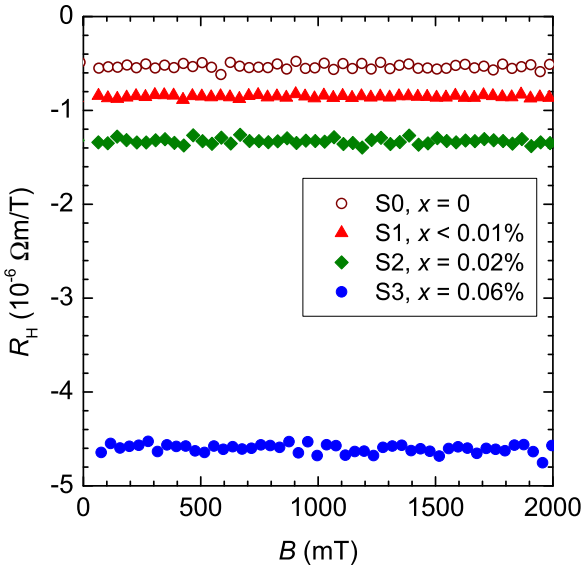

FIG. 3. (Color online) Hall coefficient $R_{\rm H} = -\partial\rho_{xy}/\partial B$ at 50 K for the studied samples. The values of the corresponding electron concentrations are given in Table I.

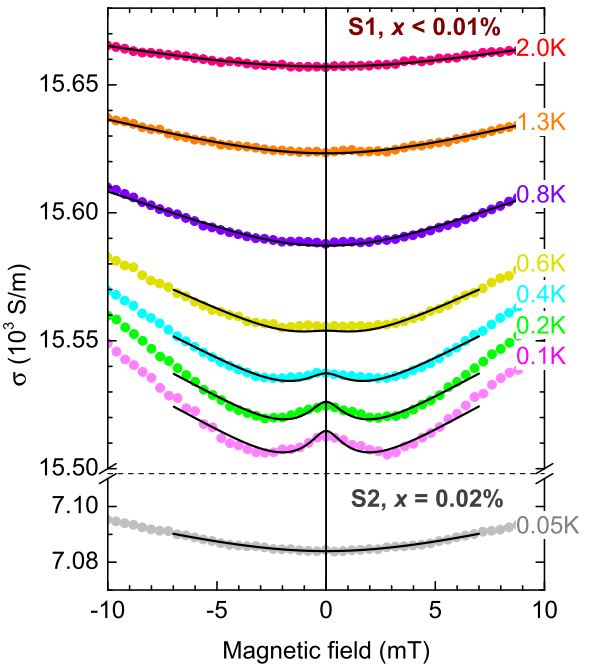

FIG. 4. (Color online) Dots: Measured magnetoconductivity for sample S1 at $T \leqslant 2$ K and for sample S2 at $T = 0.05$ K. Solid lines: Results of fitting within the theoretical 2D model treating $L_\varphi(T)$ as the only fitting parameter.

III. RESULTS

The magnitude of the conductivity $\sigma(T,B) = 1/\rho(T,B)$ has been measured at various temperatures as a function of the magnetic field applied perpendicularly to the film surface (i.e., parallel to the wz-c-axis). Since the theory of quantum localization corrections [32–34] is valid for $\omega_{c(s)}\tau k_F\ell \ll 1$ where $\hbar\omega_c$ and $\hbar\omega_s$ are the cyclotron and spin-splitting energies, respectively, and τ is the momentum relaxation time, we are interested in the range of weak magnetic fields. As seen in Fig. 4, both negative and positive MC are visible in low magnetic fields below 0.6 K for the sample S1 with the lowest Mn content, i.e., with the highest electron concentration. The negative component of MC is related to the onset of a weak antilocalization maximum, a distinct signature of spin-orbit coupling. For the samples S2 and S3 only a positive contribution to the MC is observed.

The data are analyzed with the two and three dimensional (2D and 3D, respectively) approaches developed for MC in the weakly localized regime, $k_F\ell > 1$, as the dimensional crossover condition for one-electron interference phenomena is expected to occur at relevant temperatures in our thin films. In terms of the phase coherence length $L_\varphi = (D\tau_\varphi)^{1/2}$, where $D = \hbar k_F\ell/3m^*$ is the diffusion coefficient, and τ_φ is the phase coherence time, the crossover occurs at $L_\varphi \simeq d$, where the thickness d is 150 nm for our films. At the same time, we neglect a possible crossover in the case of electron-electron interaction effects, as it occurs at lower temperatures, $L_T \simeq d$, where $L_T = (\hbar D/k_B T)^{1/2}$. We use the value of the Rashba spin-orbit coupling constant $\alpha_R = 4.5$ meV Å we determined previously for GaN:Si [37].

At first, we disregard the presence of s-d interaction; i.e., we neglect both the exchange contribution to spin-splitting and spin-disorder scattering. Therefore, $L_\varphi(T)$ is the only fitting parameter. According to the data presented in Figs. 4, 5, and 6, the 2D or the 3D model employed in the respective temperature ranges describes the experimental data very well. We have checked that if the spin-splitting is given by $\hbar\omega_s = g^*\mu_B B$, where $g^* = 1.95$ in GaN [41], one-electron localization phenomena dominate, and effects of spin-splitting upon one-electron and many-electron contributions are irrelevant to the MC.

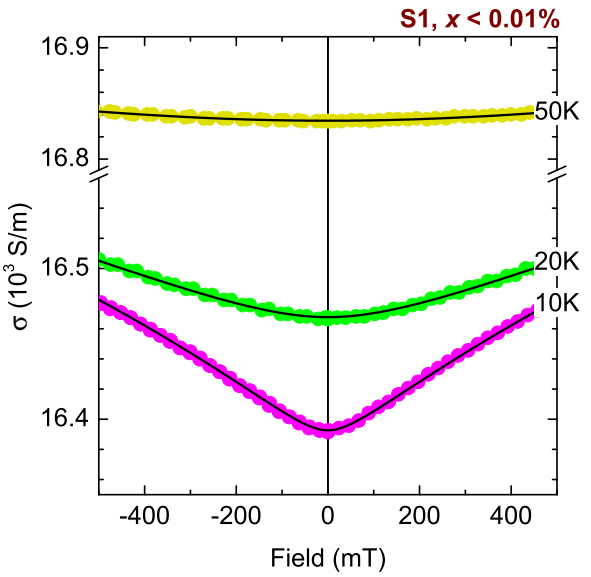

FIG. 5. (Color online) Magnetoconductivity measured for sample S1 at $T \geqslant 10$ K. Bullets: Experimental data; solid lines: theoretical fitting within the 3D theory with the phase coherence length $L_\varphi(T)$ as the only fitting parameter.

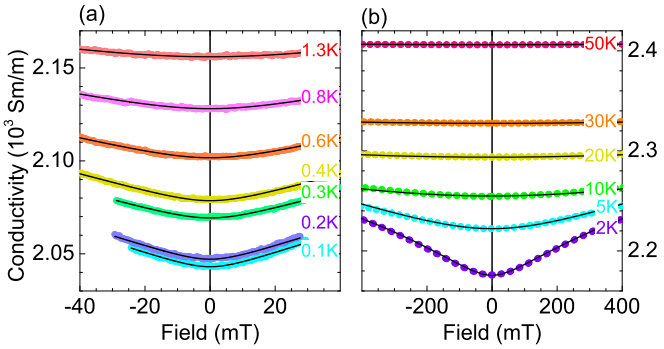

FIG. 6. (Color online) Magnetoconductivity measured for sample S3 at various temperatures. Dots: Experimental data; solid lines: theoretical fitting within the 3D theory with the phase coherence length $L_\varphi(T)$ as the only fitting parameter.

The fitted values of $L_\varphi(T)$ are summarized in Fig. 7. The data on $L_\varphi(T)$ allow us to evaluate the temperature value corresponding to the dimensional crossover for particular samples, i.e., to assess the temperature ranges at which either the 2D or the 3D theory should be applied. Actually, this information has been exploited to select the appropriate model to fit the data collected in Figs. 4, 5, and 6. Furthermore, as expected for decoherence associated with electron-electron interactions [32], we find $L_\varphi = aT^{3/4}$, where a increases with $k_F\ell$ [37]. This increase in decoherence with the approaching of the metal-insulator transition makes the effect of weak antilocalization invisible for the samples S2 and S3. Moreover, a change in the slope of $L_\varphi(T)$ is observed at about 0.3 K, which, if not caused by noise-related decoherence, may point to dimensional crossover for effects associated with electron-electron interactions, $L_T \simeq d$. Finally, the values

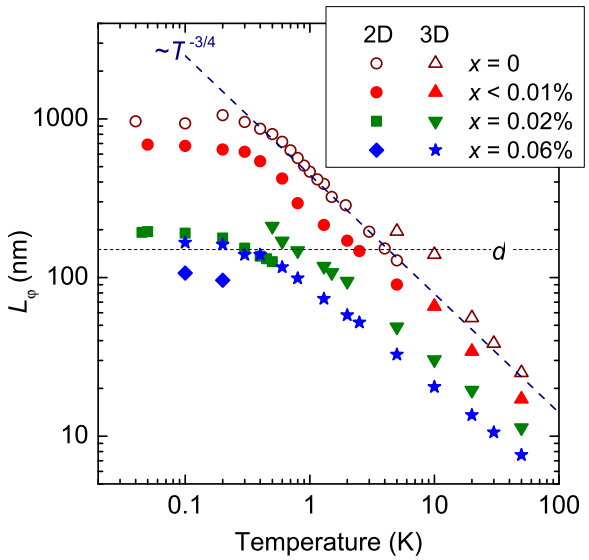

FIG. 7. (Color online) Temperature dependence of the phase coherence length L_φ obtained by fitting the magnetoconductance data for (Ga,Mn)N:Si layers within the 2D and 3D models. For comparison the corresponding data for n-GaN:Si [37] are also presented (open symbols). Dashed line: $T^{-3/4}$ dependence. The horizontal line marks the layer thickness $d = 150$ nm.

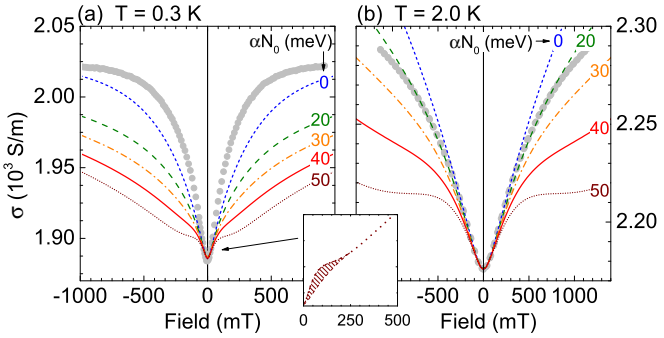

FIG. 8. (Color online) Dots: Magnetoconductivity measured for sample S3 at 0.3 K (a) and at 2 K (b). Solid lines: Values calculated for different magnitudes of $N_0\alpha$ taking the presence of Mn spins with concentration $x = 0.06\%$ into account. For $N_0\alpha \gtrsim 40$ meV a positive shoulder of magnetoconductivity (shown in the inset as a hatched area) appears in the calculations.

and the temperature dependence of L_φ indicate that spin-disorder scattering [12,42]—for which the relaxation time is independent of temperature for paramagnetic spins—is of minor importance in the case treated here.

In order to estimate an upper limit of $N_0\alpha$, we compute MC for (Ga,Mn)N:Si taking the presence of s-d exchange interaction into account. We employ the 3D model [12,32], and calculate the magnitude of MC for different values of $N_0\alpha$. In Fig. 8 the results for $T = 0.3$ K and 2 K are shown in a relatively wide field range in comparison with the experimental data for the sample S3 with the highest Mn concentration $x = 0.06\%$. The emergence of a significant negative contribution to MC, and of a kink, are seen in the simulations performed for $N_0\alpha \gtrsim 20$ and 40 meV, respectively. The absence of such features in the experimental results indicates that in (Ga,Mn)N:Si the value of $N_0|\alpha|$ is much smaller than 40 meV. Since the Mn effect scales with $x\,N_0|\alpha|$, in light of the data in Fig. 8, the conclusion that $N_0|\alpha| < 40$ meV remains valid even if we assume $x = 0.024\%$, as implied by the Hall data. Hence, our experimental results for n-(Ga,Mn)N corroborate the theoretical predictions for Mn-based III-V DMSs co-doped with shallow donors [6]. We also note that the spin-disorder scattering rate τ_s^{-1} evaluated using the standard approach [12,42] is of the order of 10^6 s^{-1}, a value much smaller than the $\tau_\varphi^{-1} \sim 10^9$ s^{-1} of our samples. However, this conclusion is valid as long as spin-disorder scattering by magnetization fluctuations associated with the carrier density fluctuations in the vicinity of the MIT is not relevant [5]. Due to the low Mn concentrations in our samples, the last contribution to spin-disorder scattering rate is expected to play a minor role.

IV. DISCUSSION AND CONCLUSIONS

We have carried out low temperature magnetotransport studies on high quality n-type wz-(Ga,Mn)N:Si films grown on a semi-insulating GaN:Mn buffer layer. The quantitative model of magnetoconductance in the weakly localized regime allows us to evaluate an upper limit for the magnitude of the s-d exchange energy and we find it to be $N_0|\alpha| < 40$ meV. This result substantiates the theoretical model [6] that assigns a reduction of the s-d exchange energy in n-type III-V

DMSs to the acceptor character of Mn in these systems. According to this model, when Mn impurities are negatively charged, they repel the conduction band electrons, with the effect of reducing the apparent magnitude of *s*-*d* coupling. Surprisingly, small magnitudes of $N_0\alpha$ were also found in studies of magnetoexcitons in semi-insulating, not *n*-type, (Ga,Mn)N [27] and (Ga,Fe)N [28]. We explain these observations with the occupation of midgap states of transition-metal ions by trapped photoelectrons under steady-state illumination, which—similarly to the case of *n*-type (Ga,Mn)N—diminishes the *s*-*d* splitting of the conduction band. In accord with this interpretation, time-resolved Kerr rotation measurements that probe the magnetic moments of conduction band electrons at times shorter than their lifetime led to the standard value of the exchange energy, $N_0\alpha = (230 \pm 20)$ meV [29].

ACKNOWLEDGMENTS

This work was supported by the Austrian Science Foundation—FWF (P22477, P24471, and P26830), by the Narodowe Centrum Nauki (Poland) through OPUS Grant No. 2013/09/B/ST3/04175, by the NATO Science for Peace Programme (Project No. 984735), and by the EU 7th Framework Programmes: CAPACITIES project REGPOT-CT-2013-316014 (EAgLE), and FunDMS Advanced Grant of the European Research Council (Grant No. 227690).

[1] J. K. Furdyna and J. Kossut, editors, *Diluted Magnetic Semiconductors*, Semiconductors and Semimetals, Vol. 25 (Academic Press, New York, 1988).

[2] T. Dietl, in *Handbook of Semiconductors*, Vol. 3B, edited by S. Mahajan (North Holland, Amsterdam, 1994), p. 1251.

[3] J. A. Gaj and J. Kossut, in *Introduction to the Physics of Diluted Magnetic Semiconductors*, Springer Series in Materials Science, Vol. 144, edited by J. A. Gaj and J. Kossut (Springer, Heidelberg, 2010), p. 1.

[4] T. Dietl and H. Ohno, Dilute ferromagnetic semiconductors: Physics and spintronic structures, Rev. Mod. Phys. **86**, 187 (2014).

[5] T. Dietl, Interplay between carrier localization and magnetism in diluted magnetic and ferromagnetic semiconductors, J. Phys. Soc. Jpn. **77**, 031005 (2008).

[6] C. Śliwa and T. Dietl, Electron-hole contribution to the apparent *s*-*d* exchange interaction in III-V dilute magnetic semiconductors, Phys. Rev. B **78**, 165205 (2008).

[7] For compilation of experimental values of $N_0\alpha$ and $N_0\beta$, see P. Kacman, Spin interactions in diluted magnetic semiconductors and magnetic semiconductor structures, Semicond. Sci. Technol. **16**, R25 (2001).

[8] T. Dietl, C. Śliwa, G. Bauer, and H. Pascher, Mechanisms of exchange interactions between carriers and Mn or Eu spins in lead chalcogenides, Phys. Rev. B **49**, 2230 (1994).

[9] K. M. Whitaker, M. Raskin, G. Kiliani, K. Beha, S. T. Ochsenbein, N. Janssen, M. Fonin, U. Rüdiger, A. Leitenstorfer, D. R. Gamelin, and R. Bratschitsch, Spin-on spintronics: Ultrafast electron spin dynamics in ZnO and $Zn_{1-x}Co_xO$ sol-gel films, Nano Lett. **11**, 3355 (2011).

[10] Hyunsoo Kim and Chul Hong Park, First-principles study of carrier-spin exchange interaction in (III,Mn)V, J. Korean Phys. Soc. **16**, 477 (2006).

[11] T. Chanier, F. Virot, and R. Hayn, Chemical trend of exchange coupling in diluted magnetic II-VI semiconductors: *Ab initio* calculations, Phys. Rev. B **79**, 205204 (2009).

[12] M. Sawicki, T. Dietl, J. Kossut, J. Igalson, T. Wojtowicz, and W. Plesiewicz, Influence of *s*-*d* exchange interaction on the conductivity of $Cd_{1-x}Mn_xSe$:In in the weakly localized regime, Phys. Rev. Lett. **56**, 508 (1986).

[13] Y. Shapira, N. F. Oliveira, P. Becla, and T. Q. Vu, Magnetoresistance and hall effect near the metal-insulator transition of *n*-type $Cd_{0.95}Mn_{0.05}Te$, Phys. Rev. B **41**, 5931 (1990).

[14] J. Jaroszyński, T. Andrearczyk, G. Karczewski, J. Wróbel, T. Wojtowicz, D. Popović, and T. Dietl, Intermediate phase at the metal-insulator boundary in a magnetically doped two-dimensional electron system, Phys. Rev. B **76**, 045322 (2007).

[15] I. P. Smorchkova, N. Samarth, J. M. Kikkawa, and D. D. Awschalom, Spin transport and localization in a magnetic two-dimensional electron gas, Phys. Rev. Lett. **78**, 3571 (1997).

[16] T. Andrearczyk, J. Jaroszyński, G. Grabecki, T. Dietl, T. Fukumura, and M. Kawasaki, Spin-related magnetoresistance of *n*-type ZnO:Al and Zn_1-xMn_xO:Al thin films, Phys. Rev. B **72**, 121309 (2005).

[17] T. Dietl, T. Andrearczyk, A. Lipińska, M. Kiecana, Maureen Tay, and Yihong Wu, Origin of ferromagnetism in Zn_{1-x} Co_xO from magnetization and spin-dependent magnetoresistance measurements, Phys. Rev. B **76**, 155312 (2007).

[18] G. M. Dalpian and S.-H. Wei, Electron-mediated ferromagnetism and negative *s*-*d* exchange splitting in semiconductors, Phys. Rev. B **73**, 245204 (2006).

[19] R. C. Myers, M. Poggio, N. P. Stern, A. C. Gossard, and D. D. Awschalom, Antiferromagnetic *s*-*d* exchange coupling in GaMnAs, Phys. Rev. Lett. **95**, 017204 (2005).

[20] M. Poggio, R. C. Myers, N. P. Stern, A. C. Gossard, and D. D. Awschalom, Structural, electrical, and magneto-optical characterization of paramagnetic GaMnAs quantum wells, Phys. Rev. B **72**, 235313 (2005).

[21] N. P. Stern, R. C. Myers, M. Poggio, A. C. Gossard, and D. D. Awschalom, Confinement engineering of *s*-*d* exchange interactions in Ga_1-xMn_xAs/$Al_y$$Ga_1$-$y$As quantum wells, Phys. Rev. B **75**, 045329 (2007).

[22] G. V. Astakhov, R. I. Dzhioev, K. V. Kavokin, V. L. Korenev, M. V. Lazarev, M. N. Tkachuk, Yu. G. Kusrayev, T. Kiessling, W. Ossau, and L. W. Molenkamp, Suppression of electron spin relaxation in Mn-doped GaAs, Phys. Rev. Lett. **101**, 076602 (2008).

[23] W. Heimbrodt, Th. Hartmann, P.J. Klar, M. Lampalzer, W. Stolz, K. Volz, A. Schaper, W. Treutmann, H.-A. Krug von Nidda, A. Loidl, T. Ruf, and V. F. Sapega, Monitoring the sign reversal of the valence band exchange integral in (Ga,Mn)As, Physica E **10**, 175 (2001).

[24] A. Kudelski, A. Lemaître, A. Miard, P. Voisin, T. C. M. Graham, R. J. Warburton, and O. Krebs, Optically probing the fine structure of a single Mn atom in an InAs quantum dot, Phys. Rev. Lett. **99**, 247209 (2007).

[25] W. Pacuski, D. Ferrand, J. Cibert, J. A. Gaj, A. Golnik, P. Kossacki, S. Marcet, E. Sarigiannidou, and H. Mariette, Excitonic giant zeeman effect in GaN:Mn^{3+}, Phys. Rev. B **76**, 165304 (2007).

[26] W. Pacuski, P. Kossacki, D. Ferrand, A. Golnik, J. Cibert, M. Wegscheider, A. Navarro-Quezada, A. Bonanni, M. Kiecana, M. Sawicki, and T. Dietl, Observation of strong-coupling effects in a diluted magnetic semiconductor $Ga_{1-x}Fe_xN$, Phys. Rev. Lett. **100**, 037204 (2008).

[27] J. Suffczyński, A. Grois, W. Pacuski, A. Golnik, J. A. Gaj, A. Navarro-Quezada, B. Faina, T. Devillers, and A. Bonanni, Effects of *s*,*p*-*d* and *s*-*p* exchange interactions probed by exciton magnetospectroscopy in (Ga,Mn)N, Phys. Rev. B **83**, 094421 (2011).

[28] J.-G. Rousset, J. Papierska, W. Pacuski, A. Golnik, M. Nawrocki, W. Stefanowicz, S. Stefanowicz, M. Sawicki, R. Jakieła, T. Dietl, A. Navarro-Quezada, B. Faina, T. Li, A. Bonanni, and J. Suffczyński, Relation between exciton splittings, magnetic circular dichroism, and magnetization in wurtzite $Ga_{1-x}Fe_xN$, Phys. Rev. B **88**, 115208 (2013).

[29] Wei-Ting Hsu, Ting-Yen Hsieh, Hsin-Feng Chen, Feng-Wen Huang, Po-Cheng Chen, Jinn-Kong Sheu, and Wen-Hao Chang, Determination of *s-d* exchange coupling in GaMnN by time-resolved kerr rotation spectroscopy, Phys. Rev. B **90**, 125205 (2014).

[30] A. Wolos, M. Palczewska, Z. Wilamowski, M. Kaminska, A. Twardowski, M. Bockowski, I. Grzegory, and S. Porowski, *s-d* exchange interaction in GaN:Mn studied by electron paramagnetic resonance, Appl. Phys. Lett. **83**, 5428 (2003).

[31] S. Barnes, Theory of electron spin resonance of magnetic ions in metals, Adv. Phys. **30**, 801 (1981).

[32] B. L. Altshuler and A. G. Aronov, in *Electron-Electron Interactions in Disordered Systems*, Modern Problems in Condensed Matter Sciences, Vol. 10, edited by A. L. Efros and M. Pollak (Elsevier, Amsterdam, 1985), pp. 1–153.

[33] H. Fukuyama, in *Electron-Electron Interactions in Disordered Systems*, Modern Problems in Condensed Matter Sciences, Vol. 10, edited by A. L. Efros and M. Pollak (Elsevier, Amsterdam, 1985), pp. 155–230.

[34] Patrick A. Lee and T. V. Ramakrishnan, Disordered electronic systems, Rev. Mod. Phys. **57**, 287 (1985).

[35] Y. Ono and J. Kossut, Anomalous magnetoconductivity in semimagnetic semiconductors showing metallic conduction, J. Phys. Soc. Jpn. **53**, 1128 (1984).

[36] J. Jaroszyński, J. Wróbel, R. Nowakowski, R. Duś, E. Papis, E. Kamińska, A. Piotrowska, G. Karczewski, T. Wojtowicz, M. Sawicki, T. Skośkiewicz, and T. Dietl, Fabrication and magnetoconductance studies on submicron wires and films of MBE-grown CdTe:In, Thin Solid Films **306**, 291 (1997).

[37] W. Stefanowicz, R. Adhikari, T. Andrearczyk, B. Faina, M. Sawicki, J. A. Majewski, T. Dietl, and A. Bonanni, Experimental determination of Rashba spin-orbit coupling in wurtzite *n*-GaN:Si, Phys. Rev. B **89**, 205201 (2014).

[38] M. A. Moram and M. E. Vickers, X-ray diffraction of III nitrides, Rep. Prog. Phys. **72**, 036502 (2009).

[39] A. Ferreira da Silva and C. Persson, Critical concentration for the doping-induced metal-nonmetal transition in cubic and hexagonal GaN, J. Appl. Phys. **92**, 2550 (2002).

[40] H. Fukuyama and K. Hoshino, Effect of spin-orbit interaction on magnetoresistance in the weakly localized regime of three-dimensional disordered systems, J. Phys. Soc. Jpn. **50**, 2131 (1981).

[41] W. E. Carlos, J. A. Freitas, M. Asif Khan, D. T. Olson, and J. N. Kuznia, Electron-spin-resonance studies of donors in wurtzite GaN, Phys. Rev. B **48**, 17878 (1993).

[42] S. Hikami, A. I. Larkin, and Y. Nagaoka, Spin-orbit interaction and magnetoresistance in the two-dimensional random system, Prog. Theor. Phys. **63**, 707 (1980).